Polyamide 66 Binary and Ternary Nanocomposites: Mechanical and Morphological Properties

Miray Mert, Ulku Yilmazer

Chemical Engineering Department, Middle East Technical University, Ankara, Turkey 06531

Received 16 July 2009; accepted 12 January 2010
DOI 10.1002/app.32112
Published online 19 May 2010 in Wiley InterScience (www.interscience.wiley.com).

ABSTRACT: Polyamide 66 (PA 66)/impact modifier blends and polyamide/organoclay binary and PA 66/organoclay/impact modifier ternary nanocomposites were prepared by the melt-compounding method, and the effects of the mixing sequences on the morphology and mechanical and flow properties were investigated. Lotader AX8840 and Lotader AX8900 were used as impact modifiers. The concentrations of the impact modifiers and the organoclay (Cloisite 25A) were maintained at 2 and 5 wt %, respectively. Both the binary and ternary nanocomposites displayed high tensile strength and Young's modulus values compared to the PA 66/impact modifier blends. Decreases occurred in the strength and stiffness of the binary nanocomposites upon incorporation of the elastomeric materials into the polymeric matrix. In general, the mixing sequence in which all three ingredients were added simultaneously and extruded twice (the All-S mixing sequence) exhibited the most enhanced mechanical properties in comparison with the mixing sequences in which two of the components were extruded in the first extrusion step and the third ingredient was added in the second extrusion step. The mechanical test results were in accordance with the organoclay dispersion. The impact strength was highly affected by the elastomeric domain sizes, interdomain distances, interfacial interactions, and organoclay delamination. The smallest elastomeric domain size was obtained for the All-S mixing sequence, whereas the elastomeric domain sizes of the other mixing sequences were quite close to each other. Drastic variations were not observed between the melt viscosities of the ternary nanocomposites prepared with different mixing sequences. © 2010 Wiley Periodicals, Inc. J Appl Polym Sci 118: 209–217, 2010

Key words: elastomers; extrusion; nanotechnology; organoclay; polyamides

INTRODUCTION

Composites find application in a wide variety of industries, such as automotive, civil construction, and aerospace.[1] The mechanical properties and heat distortion temperature can be improved through the variation of the nature and structure of the composites. Nanocomposites are a new class of composite materials that have at least one dimension in the order of a few nanometers.[2] Polymer/clay nanocomposites have especially attracted great interest because of the superior properties they display with minor amounts of clay loading (1–5 wt %).[3] The incorporation of organoclays into a polymeric matrix enhances the mechanical properties, heat distortion temperature, thermal stability, fire retardance, gas barrier properties, ionic conductivity, and optical transparency of the nanocomposites, depending on the dispersion efficiency and type of clay compatibilizers.[4,5]

Montmorillonite, saponite, and hectorite are the most commonly used layered silicates in nanocomposite preparation.[6] However, the hydrophilic structure of phyllosilicates has to be converted into an organophilic one to lower their surface energy and make them more compatible with organic polymers. Thus, hydrated cations of the interlayer are exchanged with the cationic surfactants, such as alkyl ammonium or alkyl phosphonium.[7] The structure of the nanocomposites can be classified as exfoliated, intercalated, or flocculated. In exfoliated nanocomposites, the periodic layered structure of the organoclay is destroyed, and the clay platelets are homogeneously dispersed in the polymeric matrix. In intercalated nanocomposites, the clay layers are separated from each other by 20–30 Å, and their periodic structure is preserved. Flocculated nanocomposites resemble intercalated nanocomposites, but the silicate layers can be flocculated, which arises from their hydroxylated edge–edge interactions.[4,8]

Nanocomposites can be prepared via melt compounding, solution polymerization, and *in situ* polymerization. The melt-compounding method is more suitable for polymers whose nanocomposites cannot be

Correspondence to: M. Mert (miraymert@gmail.com).
Contract grant sponsor: Scientific and Technological Research Council of Turkey; contract grant number: 104M415.

prepared by either *in situ* or solution polymerization.[4] The dispersion of the clay layers in the polymeric matrix is profoundly affected by the extruder type, screw configuration, residence time, and type and thermal stability of the components in the melt-compounding method. Elastomeric materials that function as compatibilizers and impact modifiers can also be used to increase the interfacial adhesion between the constituents, aid the delamination of the organoclay, and balance the strength and toughness of the nanocomposites, especially in the case of polyolefins.[9]

Polyamide 66 (PA 66) is an engineering thermoplastic with prominent thermal and mechanical properties, a high resistance to chemicals, and durability to fatigue and abrasion. However, it is notch-sensitive and can break easily in the presence of a crack because of its low resistance to crack propagation. Thus, it can be blended with elastomeric materials, which can considerably reduce the notch sensitivity.[10,11] Gonzáles et al.[12] prepared nanocomposites based on PA 66 and polyamide 6 (PA 6) by melt mixing and investigated the effect of PA 6 as a mediating material on PA 66 nanocomposites. The organoclay was potentially delaminated, and significant increases occurred in the modulus of elasticity and yield stress. However, the ductility increased slightly, only up to a content of 3 wt % organic montmorillonite. Yu et al.[13] reported that modified montmorillonite with more thermally stable surfactants resulted in a greater property enhancement and better durability of polymer/montmorillonite nanocomposites. Most of the organic montmorillonite layers were exfoliated in the PA 66 matrix and oriented along the injection-molding direction. Tomova and Radusch[14] toughened PA 6/PA 66 with two different types of elastomers containing maleic anhydride groups by melt compounding. Polyamide-based blends showed high elastic modulus, elongation at break, yield stress, and high impact strength values, even at low temperatures up to −20°C. The domain sizes of the elastomeric phases were larger for PA 66, which resulted from its difunctionality, which made it capable of reacting with the maleated elastomer twice per chain compared to PA 6. Liu and Wu[15] synthesized the organoclay by the co-intercalation of epoxy resin and alkyl ammonium into Na montmorillonite. The epoxy groups in the clay layers resulted in a strong interaction with PA 66, and the organoclay was dispersed homogeneously in the polymeric matrix. The mechanical properties and heat distortion temperature of the nanocomposites increased substantially.

In this study, the morphology and flow and mechanical properties of PA 66 ternary nanocomposites containing 2 wt % Cloisite 25A as an organoclay and 5 wt % Lotader AX8840 [a random copolymer of ethylene (E) and glycidyl methacrylate (GMA)] and Lotader AX8900 [a random terpolymer of E, methyl acrylate (MA), and GMA] as impact modifiers were investigated. PA 66/organoclay binary nanocomposites and PA 66/impact modifier blends were also prepared by a melt-compounding method. The mixing sequences of the components were varied to observe their effects on the degree of organoclay dispersion. Mechanical analyses, including impact and tensile tests, X-ray diffraction (XRD), scanning electron microscopy (SEM), and melt flow index (MFI) measurements, were conducted to evaluate the properties of all of the combinations and to correlate them with the organoclay delamination.

EXPERIMENTAL

Materials

PA 66 (Bergamid A65) was supplied by Polyone Co. (Istanbul, Turkey). Lotader AX8840 (E–GMA), a random copolymer of E and GMA, and Lotader AX8900 (E–MA–GMA), a random terpolymer of E, MA, and GMA, were obtained commercially from Arkema Chemicals (Columbes, France).

Cloisite 25A was purchased from Southern Clay Products (Gonzales, TX). It had a cation-exchange capacity of 95 mequiv/100 g of clay, and its organic modifier consisted of dimethyl, hydrogenated tallow, 2-ethylhexyl quaternary ammonium cation, and methyl sulfate anion.

Preparation of the PA 66 blends and nanocomposites

The PA 66 blends and binary and ternary nanocomposites were melt-compounded in a Thermoprism TSE 16 TC (Stadfordshire, UK) twin-screw, corotating, intermeshing extruder with a length/diameter ratio of 24. The organoclay and elastomer content were kept at 2 and 5 wt %, respectively. Melt compounding was carried out twice at a screw speed of 200 rpm and a feed rate of 25 g/min. The temperature profile was 260–275–275–275–280°C from the hopper to the die. The mixing sequences of the ternary nanocomposites were varied to improve the dispersion level of the organoclay in the polymeric matrix. The compounding abbreviations for these mixing sequences were All-S, CI-P, PC-I, and PI-C. In these abbreviations, C or 25A denotes the organoclay, I or IM stands for the impact modifier, and P or PA 66 indicates the polyamide. All-S (i.e., PA 66–25A–IM) is the notation used for the mixing sequence in which all the components were simultaneously melt-blended twice. In the CI-P mixing sequence [i.e., (25A/IM)–PA 66], the organoclay was first melt-compounded with the impact modifier,

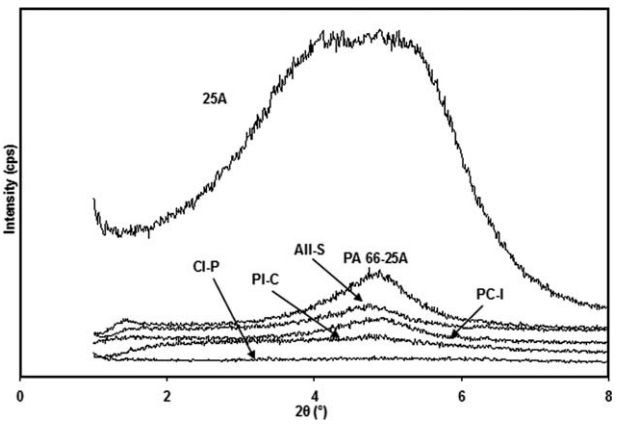

Figure 1 XRD patterns of the PA 66/Cloisite 25A/Lotader AX8840 mixing sequences.

and in the second step, this organoclay/impact modifier combination was extruded with the polymeric matrix. PC-I [i.e., (PA 66/25A)–IM] denotes the mixing sequence where polymer was first melt-mixed with the organoclay, and this mixture was melt-blended with the impact modifier in the second step. In the PI-C mixing sequence [i.e., (PA 66/IM)–25A], the polymer was melt-blended with the impact modifier in the first step and then reinforced with the organoclay in the second extrusion step. All of the components were dried *in vacuo* before processing.

Specimens were injection-molded soon after the second extrusion step with a DSM Xplore micro injection-molding instrument (Gleen, Netherlands) at a barrel temperature of 275°C and a mold temperature of 30°C. The injection-molded specimens were immediately stored in sealed polyethylene bags for at least 24 h before testing.

Characterization

XRD was carried out with a monochromatic Cu Kα radiation source (λ = 1.5418) at 40 kV and 40 mA by a Rigaku D/MAX 2200/PC X-ray diffractometer (Texas). The step size was maintained at 0.01° from 2θ = 1–8° at a 1°/min scan rate. The changes in the *d*-spacings of the organoclays were calculated by Braggs law with the shifts in the peak positions in the XRD patterns.

Impact-fractured specimens were coated with gold and etched in boiling xylene for 6 h to dissolve the elastomeric phase before their surfaces were examined by SEM analysis. The SEM micrograph of each specimen was taken at 3500× magnification, and the sizes of the elastomeric domains were calculated by an image analysis program, Image J, for 100–250 particles.

A Philips CM200 transmission electron microscope (Oregon, USA) was used for the morphological analysis of the samples at an acceleration voltage of 120 kV. Ultrathin sections 70 nm thick were cryogenically cut with a diamond knife at −100°C. The samples were trimmed parallel to the molding direction.

MFI tests (ISO 1133) were carried out with an Omega melt flow indexer at 275°C under a load of 0.325 kg. Tensile tests (ISO 527) were performed with a Lloyd LR 5K universal testing machine (West Sussex, UK) at a strain rate of 0.1/min. Notched Charpy impact tests of the specimens were carried out by a pendulum Ceast Resil Impactor (Pianezza, Italy) according to ISO 179. All the tests were conducted at 23°C, and the reported results are the averages obtained from five tested specimens.

RESULTS AND DISCUSSION

XRD analysis

The extent of intercalation or exfoliation is determined by the changes in the interlayer spacings of organoclays. A shift in the characteristic peak of the organoclay is indicative of an intercalated structure, whereas elimination of this peak demonstrates the delamination of the organoclay.[16] A decrease in the amount of intercalated clay, the breakdown of clay agglomerates, or partial exfoliation leads to reductions in the peak intensities on XRD patterns.[17] The viscosity, compounding equipment, geometry of the mixing elements, and type of the components affect the organoclay dispersion level to a great extent.[9]

XRD patterns of the PA 66 binary and ternary nanocomposites are shown in Figures 1 and 2, and the *d*-spacings of each nanocomposite type are given in Table I. The XRD patterns of the ternary nanocomposites given in Figure 2 belong to PA 66–25A–8840 combinations, whereas Figure 3 shows the XRD patterns of PA 66–25A–8900 combinations. The presence of the main peak and a diffraction peak, which shifted to lower 2θ angles, in the XRD patterns was related to the presence of a region composed of unintercalated organoclay or d_{002} of interlayer distance d_{001}.[16] Changing the mixing sequence and the

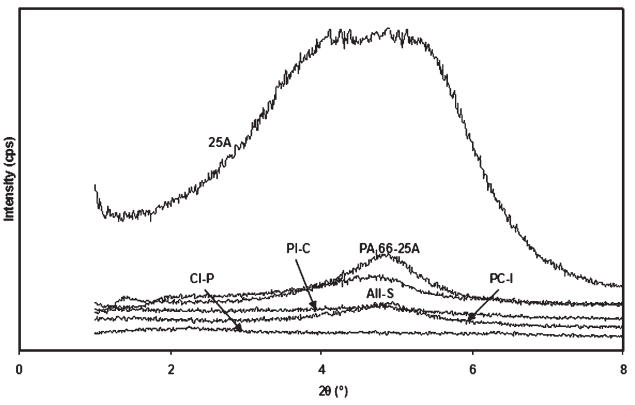

Figure 2 XRD patterns of the PA 66/Cloisite 25A/Lotader AX8900 mixing sequences.

TABLE I
XRD Results

Component	Peak I		Peak II	
	d-spacing (Å)	2θ (°)	*d*-spacing (Å)	2θ (°)
Organoclay				
Cloisite 25A	18.0	4.90	—	—
PA 66 binary nanocomposite				
PA 66–25A	63.1	1.40	18.6	4.74
PA 66 ternary nanocomposites				
PA 66–25A–8840 (All-S)	52.9	1.67	18.7	4.73
PA 66–25A–8900 (All-S)	44.4	1.99	19.0	4.64
Mixing sequences of PA 66 ternary nanocomposites				
(25A/8840)–PA 66 (CI-P)	—	—	—	—
(PA 66/25A)–8840 (PC-I)	53.2	1.66	18.8	4.70
(PA 66/8840)–25A (PI-C)	43.7	2.02	18.6	4.74
(25A/8900)–PA 66 (CI-P)	39.1	2.26	—	—
(PA 66/25A)–8900 (PC-I)	18.7	4.72	—	—
(PA 66/8900)–25A (PI-C)	18.8	4.71	—	—

incorporation of the elastomeric materials into the polymeric matrix aided the delamination of the organoclay. It was apparent from the *d*-spacings of the nanocomposites that the degree of organoclay dispersion was better in the presence of Lotader AX8840 (E–GMA) and Lotader AX8900 (E–MA–GMA). However, in some of the mixing sequences of the PA 66 nanocomposites, relatively small intensities of the shoulders at lower 2θ angles, in comparison with the intensity of the main peak, corroborated that one or more polymer chains penetrated between the clay galleries without achieving complete separation. Although there were a few exfoliated structures, the organoclay was mostly intercalated or in the form of tactoids in these nanocomposites.[18]

It was obvious in the XRD patterns that there was an intercalated region in almost all of the nanocomposites. The *d*-spacings of the nanocomposites were generally higher compared to the organoclay; this showed that the organoclay was well dispersed in the polymeric matrix. The organoclay was fully delaminated in the CI-P mixing sequence of the PA 66 nanocomposites containing Lotader A X8840, whereas it was mostly in the intercalated form in the nanocomposites prepared with the CI-P mixing sequence containing Lotader AX8900. Although we expected to obtain a better dispersion in the CI-P and PI-C mixing sequences, because of their high viscosities, the *d*-spacings of the PI-C mixing sequences were relatively smaller or similar to the PC-I mixing sequences. This resulted from the fact that the extrusion of the polymeric matrix with the organoclay only once was insufficient for the homogeneous dispersion of the organoclay in the PI-C mixing sequence, despite its high viscosity, which could increase the shear intensity applied on the clay platelets. Exfoliation of the clay platelets was obvious from the transmission electron microscopy (TEM) analysis of the All-S mixing sequence that contained Lotader AX8900 and is shown in Figure 3. Thin black lines indicate the clay layers, whereas white regions represent the elastomeric domains. Interaction of both the organoclay and the impact modifier with the polymeric matrix helped in their homogeneous dispersion.

Functional groups of E–GMA and E–BA–GMA also increased the interfacial interactions taking place between the organic modifier, clay surface, and polymeric matrix. For instance, GMA groups could react with both the acid and amine ends of the polymeric matrix, and ester groups present in the structure of acrylates could react with the terminal amino groups.[19,20] Organoclay exfoliation is also a function of variety of factors including the packing density of the organoclay, interactions between the components, shear intensity, and organic modifier polarity.

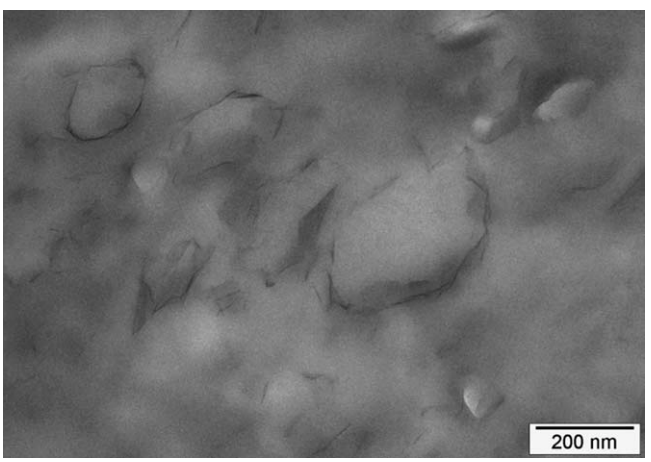

Figure 3 TEM micrograph of the PA 66/Cloisite 25A/Lotader AX8900 (All-S) mixing sequence.

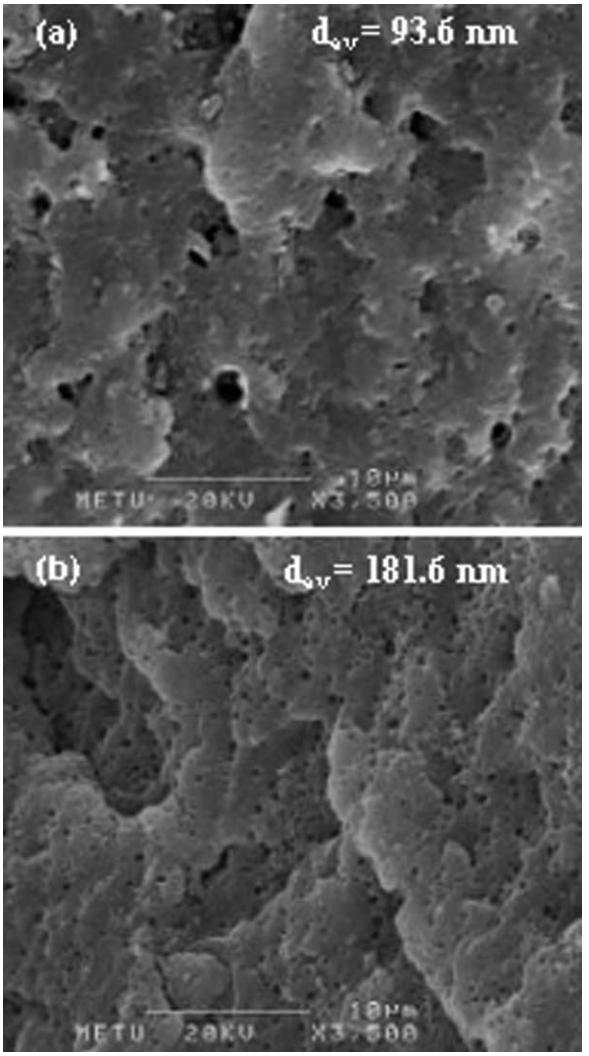

Figure 4 SEM micrographs of the PA 66/impact modifier blends: (a) 5 wt % Lotader AX8840 (3500×) and (b) 5 wt % Lotader AX8900 (3500×).

SEM analysis

The impact-fractured surfaces of the specimens were examined by SEM, and the sizes of the elastomeric domains were calculated with the image analysis program, Image J. Average diameter of the elastomeric domains (d_{av}) are given on SEM micrographs. The SEM micrographs of the PA 66 blends are shown in Figure 4, whereas the SEM micrographs of the ternary nanocomposites prepared by the All-S method and the binary nanocomposites are shown in Figure 5. The SEM micrographs of the PA 66 ternary nanocomposites prepared by the CI-P, PC-I, and PI-C mixing sequences are given in Figures 6 and 7.

To obtain a fine dispersion, a good balance had to be set between the viscosity and melt elasticity of the components, and a certain level of grafting of the dispersed phase was essential to reduce the interfacial tension and to increase the adhesion between the phases. To increase the toughness, a uniform distribution of the elastomeric domains, an appropriate range of the elastomeric domain size and interdomain distance, and a low modulus ratio

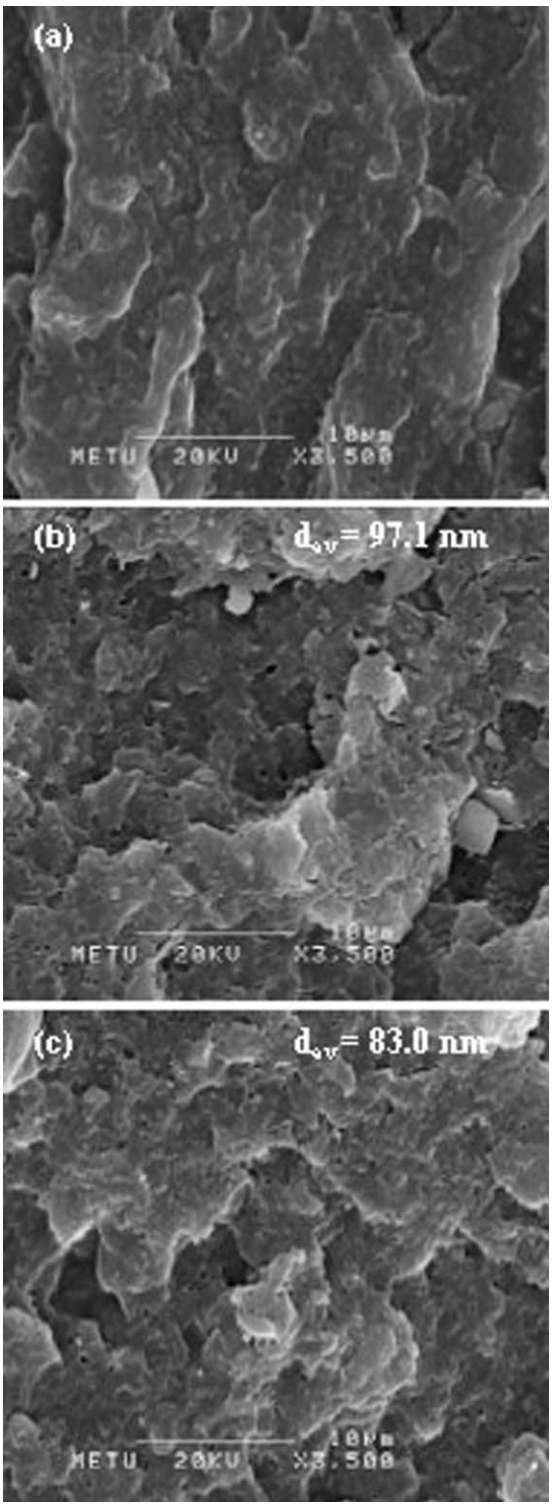

Figure 5 SEM micrographs of (a) the PA 66/Cloisite 25A binary nanocomposite (3500×) and (b,c) the PA 66/Cloisite 25A/impact modifier (All-S) ternary nanocomposites with Lotader AX8840 (3500×) and Lotader AX8900 (3500×), respectively.

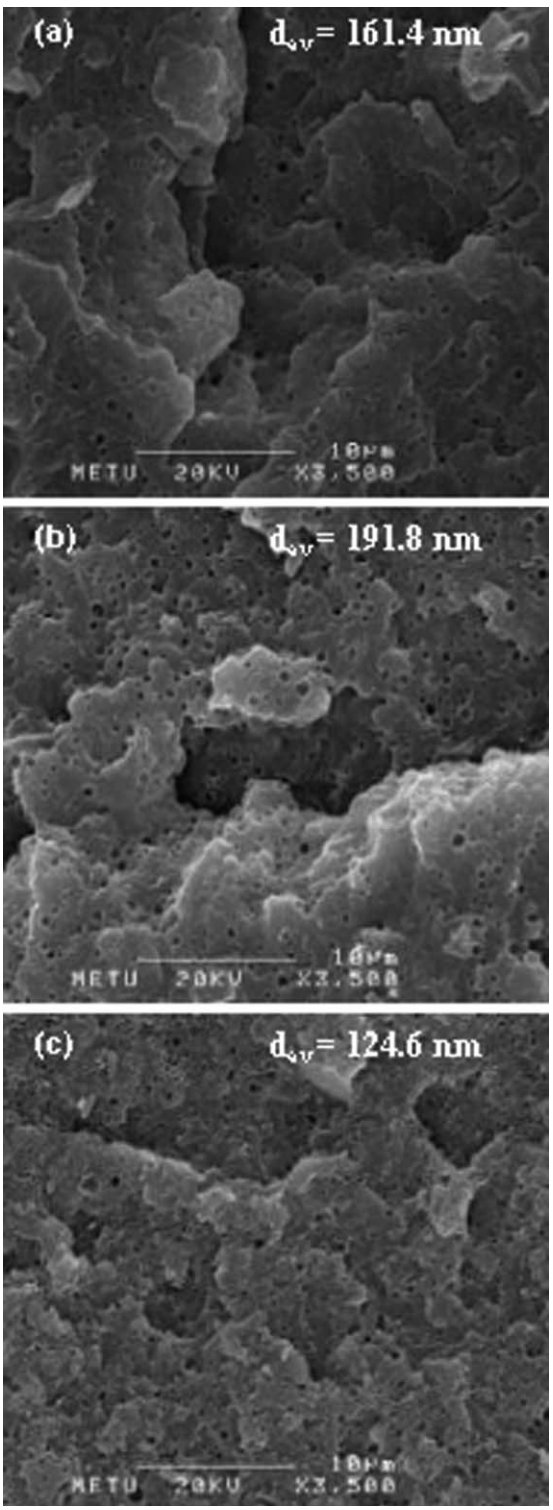

Figure 6 SEM micrographs of the PA 66/Cloisite 25A/Lotader AX8840 mixing sequences: (a) CI-P (3500×), (b) PC-I (3500×), and (c) PI-C (3500×).

between the elastomer and polyamide bulk phases were required. The molecular weight of the matrix, melt elasticity of the components, shear intensity, mobility of the interface, and surface tension all controlled the domain sizes because a lower tension impeded the coalescence of the elastomeric domains because of the immobilizing effect of the chemical reactions forming interfacial copolymers.[18] Organoclay platelets exfoliated in the polymeric matrix

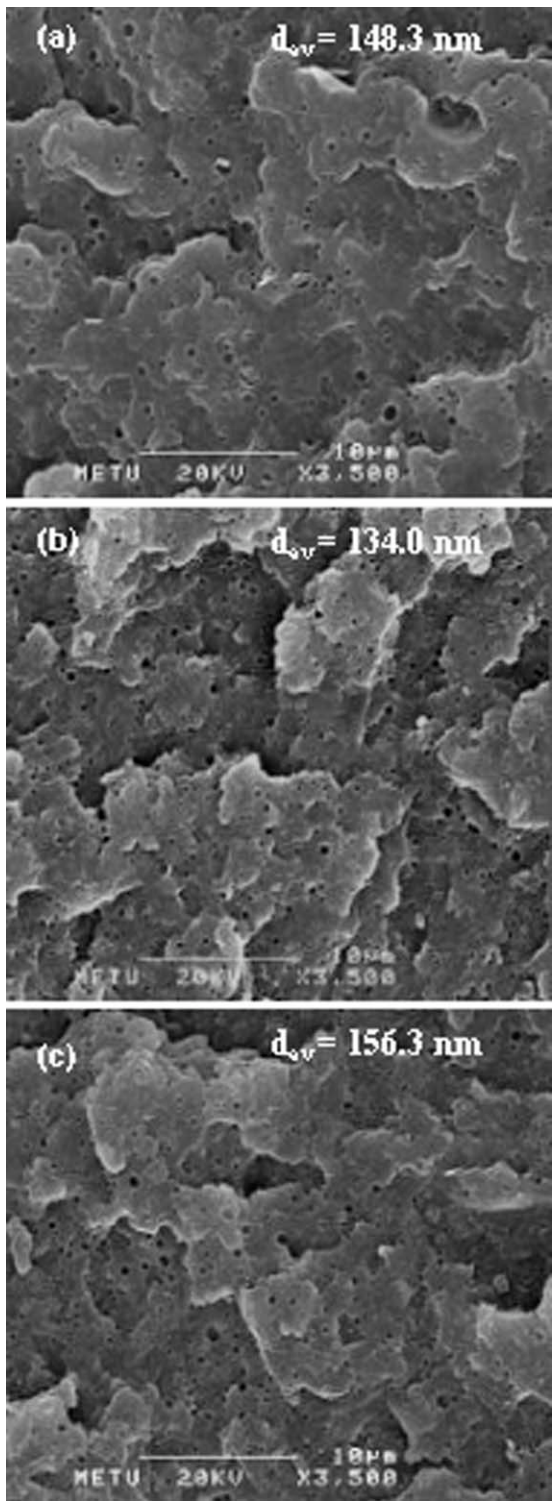

Figure 7 SEM micrographs of the PA 66/Cloisite 25A/Lotader AX8900 mixing sequences: (a) CI-P (3500×), (b) PC-I (3500×), and (c) PI-C (3500×).

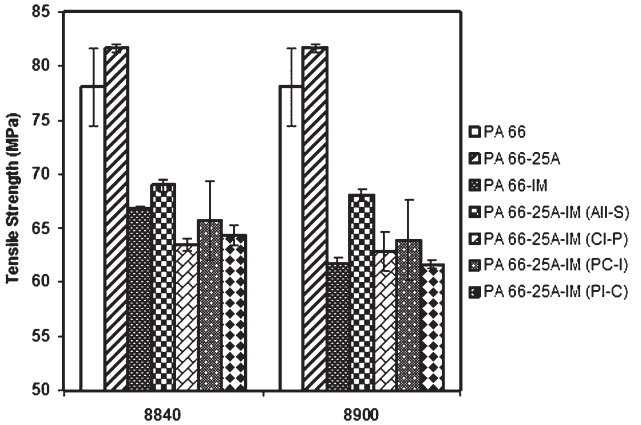

Figure 8 Tensile strength of the PA 66/Cloisite 25A/impact modifier mixing sequences.

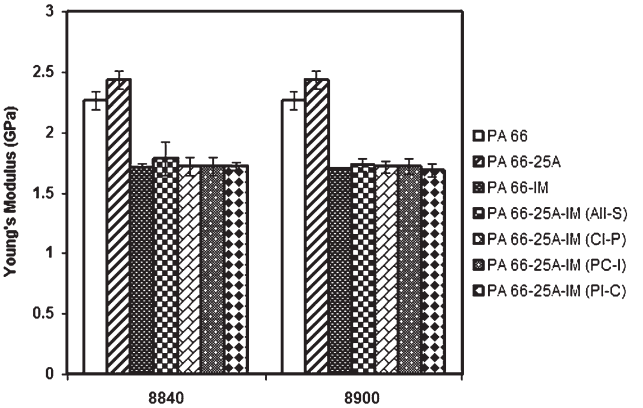

Figure 9 Young's modulus of the PA 66/Cloisite 25A/impact modifier mixing sequences.

functioned as barriers and hindered the coalescence of the elastomeric domains.[21]

It could be inferred from the SEM micrographs that no clay agglomeration occurred in the PA 66 nanocomposites. The elastomeric domain sizes were expected to be larger in the blends compared to the nanocomposites. However, the elastomeric domain sizes were found to be slightly larger in the All-S ternary nanocomposites containing Lotader AX8840 (E–GMA) in comparison with the blends. This could have stemmed from the interaction of the organoclay with the impact modifier, which retarded the reductions in the elastomeric domain sizes and their dispersion in the polymeric matrix.[22] The domain sizes of the All-S mixing sequences were smaller than the domain sizes of the CI-P, PC-I, and PI-C mixing sequences. In fact, it was more probable to obtain smaller elastomeric domain sizes for the PI-C and CI-P mixing sequences because of the high viscosity of the impact modifier, which increased the shear intensity. Large domain sizes in materials prepared by the PI-C mixing sequences were ascribed to the extrusion of the organoclay with the polymeric matrix and the impact modifier only once. The clay platelets could not act as stabilizing agents for increasing the interfacial adhesion because, in the PI-C mixing sequence, the organoclay met the other components only in the second extrusion step. The elastomeric domain sizes were also relatively large for the materials prepared by the PC-I mixing sequence, and this was attributed to the melt compounding of the impact modifier with the polymer–organoclay combination only during the second extrusion step. The shear intensity applied on the impact modifier in a single extrusion step was not capable of breaking up the elastomeric domains. On the other hand, the interactions of the elastomeric phase with the organoclay were more severe in the case of the CI-P mixing sequence, which inhibited the reductions in the domain sizes, because the organoclay was initially melt-mixed with the impact modifier.

Thus, it was significant to melt-compound all of the components simultaneously to obtain domain sizes within a specific range that could produce enhanced toughness levels. The interactions between the components were not minimized, and the same shear intensity was applied to all of the components in both of the processing steps in the All-S mixing sequence.

Mechanical properties

The mechanical properties of the PA 66 blends and nanocomposites were determined by tensile and impact tests, and the results of these tests were correlated with the interaction between the components, dispersion level of the organoclay, and elastomeric materials and the elastomeric domain sizes. Tensile strength, Young's modulus, and elongation at break (%) values of the blends and binary and ternary nanocomposites are compared in Figures 8–10 for all of the mixing sequences. The impact strength results of all of the combinations are shown in Figure 11.

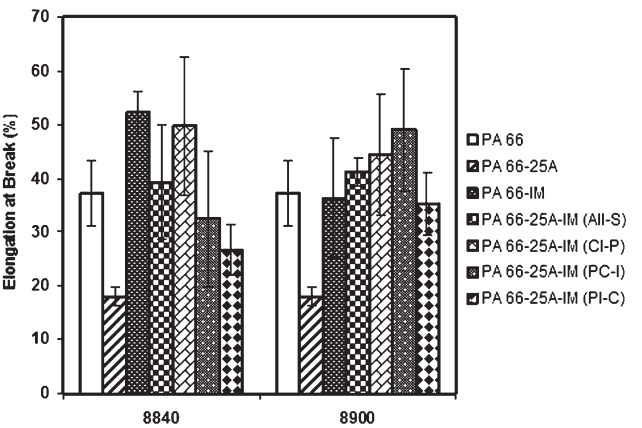

Figure 10 Elongation at break (%) of the PA 66/Cloisite 25A/impact modifier mixing sequences.

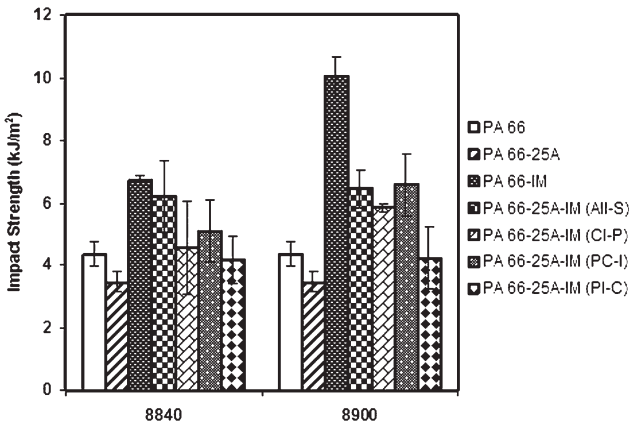

Figure 11 Impact strength of the PA 66/Cloisite 25A/impact modifier mixing sequences.

The tensile strength and Young's modulus decreased upon addition of the impact modifiers to the polymeric matrix. On the other hand, the elongation at break (%) values of the blends were higher than those of the nanocomposites because the elastomeric materials acted as stress concentrators, and yielding or crazing around the elastomeric domains increased the energy absorption during crack formation. As the plastic deformation mechanism involved dilatational strain, the yield strength of the blends decreased, whereas the elongation at break (%) values became higher.[18] Inorganic silicate particles stiffened the matrix and increased the tensile strength and Young's modulus, whereas the elongation at break became lower with increasing organoclay content. The reinforcement effect was caused by the high aspect ratio of the silicate particles, which created a large contact area with the polymeric matrix.[21] However, external stresses could not strain the silicate particles. The tie chain amount between the crystalline areas was also reduced in the nanocomposites, and stress could not be transferred through the sample, which led to early failure.[23] Interactions between the components were also highly effective in increasing the strength and stiffness of the materials because stress could not be transferred as soon as the physical union formed during blending was overcome.[18]

The All-S mixing sequence exhibited the highest tensile test results because all of the components underwent the same mixing history, as discussed earlier. On the other hand, in the PI-C mixing sequence, the organoclay was melt-compounded with the polymer/impact modifier blend only once in the second extrusion step. Thus, complete delamination of the organoclay platelets could not be achieved because of the insufficient shear intensity to tear the clay layers apart. Extrusion of the organoclay twice with the other components resulted in better delamination of the clay platelets. Thus, the highest tensile strength and Young's modulus were observed in the nanocomposites prepared by the All-S mixing sequence, and it was typically followed by the PC-I, CI-P, and PI-C mixing sequences. The elongation at break (%) values were higher for the CI-P, PC-I, and All-S mixing sequences compared to the PI-C mixing sequence.

The trend observed for the tensile test results of all of the combinations was also valid for the impact test results. The lowest impact test results were obtained for the PI-C mixing sequence, and the highest results were obtained for the All-S mixing sequence. Toughness decreased as the organoclay was incorporated into the polymeric matrix, as opposed to the addition of impact modifiers. The impact strength of the ternary nanocomposites was highly improved, as shown by the low values obtained for the binary nanocomposites. The effect of the impact modifier was more pronounced on the resultant properties in comparison with the effect of the organoclay because the concentration of the impact modifier was higher than the concentration of the organoclay in the polymeric matrix. The impact strength was also highly affected by the elastomeric domain sizes, interdomain distances, and interfacial adhesion between the phases. There were no significant variations between the impact strength values belonging to the combinations that contained two different types of impact modifiers.

The presence of the functional groups in the chemical structure of the impact modifiers promoted a morphology composed of fine elastomeric domains. As the sizes of the elastomeric domains got smaller or larger than an appropriate range, the resistance of the materials to crack propagation became lower. Thus, the type of the components, the organoclay dispersion, and the interactions at the interface, which stabilized the matrix, resulted in changes in the domains sizes, interdomain distances, and mechanical test results.

MFI analysis

The decreases in MFI increased the shear intensity and aided the dispersion of the organoclay in the polymeric matrix. The MFI results shown in Table II indicate that there was not much difference between the melt viscosities of the neat PA 66 matrix and the one that was extruded twice. Thus, the change that may have occurred in the molecular weight of the polymeric matrix during both of the processing steps was ignored when the MFI analysis results were evaluated. The slight decrease in the molecular weight of the polymeric matrix did not significantly contribute to the changes in the melt viscosities of the blends and the nanocomposites.

TABLE II
MFI Results for All of the Compositions

Component	PA 66 concentration (wt %)	MFI (g/10 min)
Polyamides		
PA 66 (not extruded)	100	16.4 ± 1.6
PA 66 (twice extruded)	100	16.3 ± 1.0
Impact modifiers		
Lotader AX8840	—	5.4 ± 0.2
Lotader AX8900	—	3.8 ± 0.2
PA 66 impact modifier blends		
PA 66–8840	95	11.6 ± 3.0
PA 66–8900	95	11.8 ± 1.6
PA 66 binary nanocomposite		
PA 66–25A	98	18.7 ± 1.4
PA 66 ternary nanocomposites		
PA 66–25A–8840 (All-S)	93	8.5 ± 0.3
PA 66–25A–8900 (All-S)	93	8.5 ± 0.2
Mixing sequences of PA 66 ternary nanocomposites		
(25A/8840)–PA 66 (CI-P)	93	11.9 ± 0.5
(PA 66/25A)–8840 (PC-I)	93	12.3 ± 0.7
(PA 66/8840)–25A (PI-C)	93	11.8 ± 0.5
(25A/8900)–PA 66 (CI-P)	93	11.1 ± 1.6
(PA 66/25A)–8900 (PC-I)	93	12.3 ± 0.4
(PA 66/8900)–25A (PI-C)	93	11.1 ± 0.4

The MFI values of the neat impact modifiers were lower than the MFI of PA 66. Thus, in Table II, decreases in the MFI of the blends can be observed and compared to the MFI of the PA 66 matrix. The MFI of the binary nanocomposites was slightly higher than the MFI of PA 66. This was associated with the slip between the PA 66 matrix and the oriented clay layers during high shear flow.[24,25] Large differences were not observed between the melt viscosities of the ternary nanocomposites prepared with different mixing sequences. However, the melt viscosity was somewhat higher for the nanocomposites prepared by the PI-C and CI-P mixing sequences.

CONCLUSIONS

The morphology and mechanical and flow properties of the nanocomposites were affected by the organoclay dispersion, elastomeric domain size, mixing sequence, and interactions taking place between the organic modifier and the clay surface and between the polymeric matrix and the impact modifier. Decreases in the tensile strength and Young's modulus of the blends were compensated by the addition of the organoclay in the ternary nanocomposites. Although the strength and stiffness of the binary nanocomposites were high (82 MPa), their elongation at break (18%) and toughness results (3.5 kJ/m^2) were quite low. Thus, the toughness and strength of the materials could be balanced by preparation of ternary nanocomposites, whose impact (4.2–6.6 kJ/m^2) and tensile test results (62–69 MPa) were not significantly lower compared to those of the PA 66/impact modifier blends and the PA 66/organoclay binary nanocomposites. Organoclay dispersion was good in almost all of the nanocomposites, as shown by the XRD results. However, the mechanical test results of the All-S and PC-I mixing sequences were slightly higher than the results of other mixing sequences. The elastomeric domain sizes of the nanocomposites prepared by the CI-P, PC-I, and PI-C mixing sequences were similar to each other, although lower values were obtained for the All-S mixing sequence. Increases in the elastomeric domain sizes had adverse effects on the toughness values. Thus, because of the interactions between the constituents and the shear intensity applied in both of the extrusion steps, it was more advantageous to melt-mix all of the components simultaneously.

References

1. Chawla, K. Composite Materials Science and Engineering, 2nd ed.; Springer-Verlag: New York, 1998.
2. Varlot-Masenelli, K.; Reynaud, E.; Vigier, G.; Varlet, J. J Polym Sci Part B: Polym Phys 2002, 40, 272.
3. Chiu, F. C.; Lai, S. M.; Chen, Y. L.; Lee, T. H. Polymer 2005, 46, 11600.
4. Ray, S. S.; Okamoto, M. Prog Polym Sci 2003, 28, 1539.
5. Baldi, F.; Bignotti, F.; Tieghi, G.; Riccó, T. J Appl Polym Sci 2006, 99, 3406.
6. Tjong, S. C.; Bao, S. P. J Polym Sci Part B: Polym Phys 2005, 43, 585.
7. Alexandre, M.; Dubois, P. Mater Sci Eng 2000, 28, 1.
8. Sikdar, D.; Katti, D. R.; Katti, S. K.; Bhowmik, R. Polymer 2006, 47, 5196.
9. Gianelli, W.; Camino, G.; Dintcheva, N. T.; Verso, S. L.; La Mantia, F. P. Macromol Mater Eng 2004, 289, 238.
10. Mark, H. F.; Bilakes, N.; Overberger, C. G.; Menges, G. Encyclopedia of Polymer Science and Technology, 3rd ed.; Wiley-Interscience: Hoboken, NJ, 2003.
11. Kohan, M. I. Nylon Plastics; Wiley: New York, 1973.
12. Gonzáles, I.; Eguiazábal, J. I.; Nazábal, J. Compos Sci Technol 2006, 66, 1833.
13. Yu, Z. Z.; Yang, M.; Zhang, Q.; Zhao, C.; Mai, Y. W. J Polym Sci Part B: Polym Phys 2003, 41, 1234.
14. Tomova, D.; Radusch, H. J. Polym Adv Technol 2003, 14, 19.
15. Liu, X.; Wu, Q. Macromol Mater Eng 2002, 287, 180.
16. Xu, W.; Liang, G.; Wang, W.; Tang, S.; He, P.; Pan, W. P. J Appl Polym Sci 2003, 88, 3225.
17. Chang, J.; An, Y. U. J Polym Sci Part B: Polym Phys 2002, 40, 670.
18. Contreras, V.; Cafiero, M.; Da Silva, S.; Rosales, C.; Perera, R.; Matos, M. Polym Eng Sci 2006, 46, 1111.
19. Tedesco, A.; Krey, P. F.; Barbosa, R. V.; Mauler, R. S. Polym Int 2001, 51, 105.
20. Raval, H.; Devi, S.; Singh, Y. P.; Mehta, M. H. Polymer 1991, 32, 493.
21. Hassan, A.; Othman, N.; Wahit, M. U.; Wei, L. J.; Rahmat, A. R.; Ishak, Z. A. M. Macromol Symp 2006, 239, 182.
22. Dasari, A.; Yu, Z. Z.; Yang, M.; Zhang, Q. X.; Xie, X. L.; Mai, Y. W. Compos Sci Technol 2006, 66, 3097.
23. Vlasveld, D. P. N.; Vaidya, S. G.; Bersee, H. E. N.; Picken, S. J. Polymer 2005, 46, 3452.
24. Cho, J. W.; Paul, D. R. Polymer 2001, 42, 1083.
25. Gonzáles, I.; Eguiazábal, J. I.; Nazábal, J. Polymer 2005, 46, 2978.